# Origin of supposedly biogenic magnetite in the Martian meteorite Allan Hills 84001

**David J. Barber*† and Edward R. D. Scott‡**

*Advanced Materials Department, School of Industrial and Manufacturing Science, Cranfield University, Cranfield MK43 0AL, and School of Chemical and Life Sciences, University of Greenwich, London SE18 6PF, United Kingdom; and ‡Hawai'i Institute of Geophysics and Planetology, University of Hawai'i at Manoa, Honolulu, HI 96822

Edited by John A. Wood, Harvard-Smithsonian Center for Astrophysics, Cambridge, MA, and approved March 19, 2002 (received for review January 25, 2002)

**Crystals of magnetite ($Fe_3O_4$) and periclase (MgO) in Fe-Mg-Ca carbonate in the Martian meteorite Allan Hills 84001 were studied by using transmission electron microscopy to understand their origin and evaluate claims that the magnetites were made by Martian microorganisms. In magnesian carbonate, periclase occurs as aggregates of crystals (grain size ≈3 nm) that are preferentially oriented with respect to the carbonate lattice. Larger periclase crystals ≈50 nm in size are commonly associated with voids of similar size. Periclase clearly formed by precipitation from carbonate as a result of partial decomposition and loss of $CO_2$. Magnetite occurs in more ferroan carbonate, and, like periclase, it is associated with voids and microfractures and the two oxides may be intermixed. Magnetite nanocrystals that are commonly euhedral and entirely embedded in carbonate are topotactically oriented with respect to the carbonate lattice, showing that they formed as solid-state precipitates. Magnetites in Fe-rich carbonate rims are not well oriented. These magnetites are generally more irregular in shape and diverse in size than the euhedral variety. All occurrences of magnetite and periclase are entirely consistent with *in situ* growth by solid-state diffusion as a result of carbonate decomposition during impact heating. Biogenic sources should not be invoked for any magnetites.**

Nanocrystals of magnetite ($Fe_3O_4$) inside 3.9-Gyr-old (1) carbonate in Martian meteorite Allan Hills (ALH) 84001 contain a record of the ancient Martian magnetic field (2) and possible evidence for fossil Martian life (3). Two recent studies have advanced the claim that the magnetites were made by microorganisms. Thomas-Keprta *et al.* (4) used transmission electron microscopy (TEM) to study magnetites obtained by dissolving carbonates in acid. They found that about 25% were shaped like elongated prisms (later called "truncated hexa-octahedrons" (5), and had sizes (4–100 nm), shapes, structures, and compositions that appeared to be indistinguishable from those produced by one strain of magnetotactic bacteria. Because terrestrial inorganic magnetites have very different properties, they inferred that the Martian magnetites were biological in origin and constitute evidence of the oldest life yet found. In the second study, Friedmann *et al.* (6) examined broken rock surfaces and identified what they interpreted as chains of magnetite crystals like those in modern magnetotactic bacteria.

Both these claims for fossil life have been disputed. Buseck *et al.* (7) questioned the identification of magnetite by Friedmann *et al.* (6) and noted that intact magnetite chains from magnetotactic bacteria were unlikely to survive in rocks. Buseck *et al.* (7) found that magnetites from three different strains of bacteria had different shapes and criticized the techniques used by Thomas-Keprta *et al.* (4, 5) to select magnetite crystals and to study their shapes. They also argued that the crystal size distributions of bacterial and meteoritic magnetites appeared to be different. Although Buseck *et al.* (7) recognized that the similarities between the Martian and bacterial magnetites are intriguing, they, like Treiman,§ inferred that strong evidence for biogenic Martian magnetites was lacking. Buseck *et al.* (7) called for more detailed studies of the shapes of the Martian magnetite crystals to resolve this issue.

Arguments against a biogenic origin for magnetites in ALH 84001 were previously advanced by Bradley *et al.* (8, 9). Their TEM studies showed that whisker-like magnetites had grown epitaxially on a carbonate fracture surface so that two crystal lattices were closely aligned at their interface. They concluded that these magnetites had condensed from a vapor above 120°C. However, Thomas-Keprta *et al.* (4) pointed out that the whisker-like magnetites, which comprised 7% of their sample, were found only in the interiors of carbonate grains. They inferred that the elongated prismatic magnetites, which they suggested were biogenic, are largely located in the optically opaque rims where epitaxial relationships are not observed. Four other origins have been suggested for some or all of the magnetite in ALH 84001: deposition of abiogenic grains that formed elsewhere (4, 5), thermal oxidation of sulfides (9), precipitation from aqueous solutions,¶ and *in situ* formation because of shock-induced, thermal decomposition of carbonate (‖, 10–12).

We have performed TEM studies of the ALH 84001 magnetites and their associated carbonate, silicate, oxide, and sulfide minerals *in situ*. Here, we focus solely on results that bear on the origin of the magnetite.

## Methods

Minerals and glasses in typical locations were characterized by TEM imaging, x-ray microanalysis, and electron diffraction, taking note of their morphologies, internal microstructures, compositions, and spatial interrelationships. Our specimen was a doubly polished thin section (ALH 84001,353) supplied by the National Aeronautics and Space Administration (NASA) Johnson Space Center. We approached the controversial origin of the carbonates in ALH 84001 from a perspective gained from TEM studies of carbonates of many types (e.g., refs. 13–16). Carbonate-bearing areas were identified by optical microscopy and examined by using Zeiss DSM-962 and Hitachi (Tokyo) S-800 field emission scanning electron microscopes. The section was then demounted, and pieces of it were glued to coarse 3-mm-diameter copper grids with epoxy resin. To make TEM speci-

This paper was submitted directly (Track II) to the PNAS office.

Abbreviations: TEM, transmission electron microscopy; ALH, Allan Hills.

†To whom reprint requests should be addressed. E-mail: DavidBarber@dbmatcon.demon.co.uk.

§Treiman, A. H. (2001) in *Proceedings of the 32nd Lunar and Planetary Science Conference* [CD-ROM] (Lunar and Planetary Institute, Houston), no. 1304 (abstr.).

¶Blake, D., Treiman, A., Cady, S., Nelson, C. & Krishnan, K. (1998) in *Proceedings of the 29th Lunar and Planetary Science Conference* [CD-ROM] (Lunar and Planetary Institute, Houston), no. 1347 (abstr.).

‖Brearley, A. J. (1998) in *Proceedings of the 29th Lunar and Planetary Science Conference* [CD-ROM] (Lunar and Planetary Institute, Houston), no. 1451 (abstr.).

The publication costs of this article were defrayed in part by page charge payment. This article must therefore be hereby marked "*advertisement*" in accordance with 18 U.S.C. §1734 solely to indicate this fact.



www.pnas.org/cgi/doi/10.1073/pnas.102045799

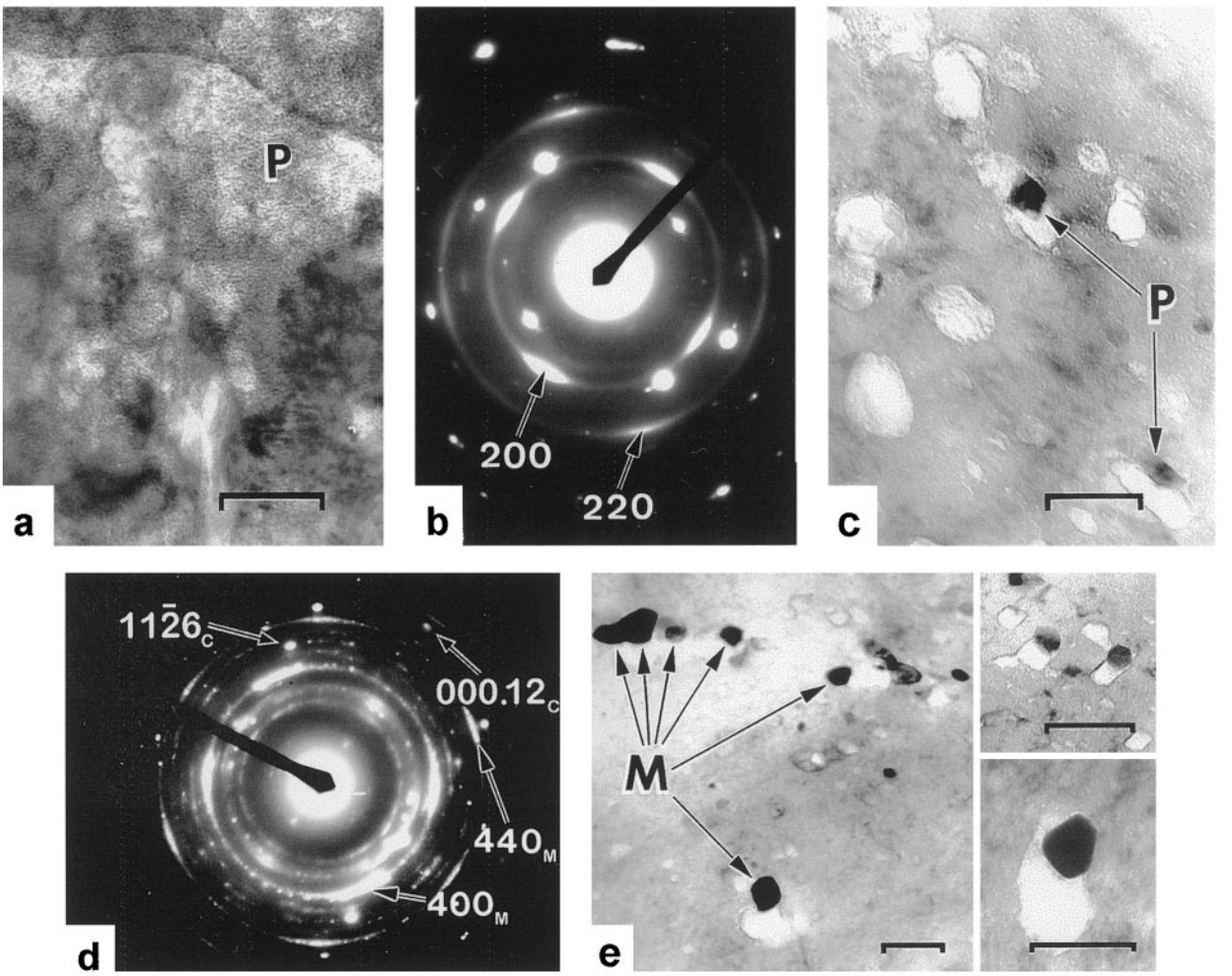


**Fig. 1.** TEM images of periclase and magnetite in carbonate and their electron diffraction patterns: (*a*) nano-crystalline aggregate of periclase (P) in foamy region of magnesian carbonate; (*b*) diffraction pattern from *a*: 200 and 220 rings for MgO are prominent and show weak 001 preferred orientation; spot reflections are from carbonate; (*c*) two MgO crystals (P) associated with voids in magnesian carbonate; (*d*) diffraction pattern from magnetite-rich rim showing magnetite rings indicating preferred orientation (400 and 440 rings are marked) and spot reflections mostly from carbonate, which form an incomplete $<1\bar{1}00>$ zone axis pattern; (*e*) examples of euhedral crystals of magnetite, the larger ones mostly associated with voids in ferroan carbonate. Scale bars = 100 nm.

mens, we utilized an Ion Tech (Teddington, U.K.) beam-milling system with FAB (fast atom beam) sources, operating at 5 kV with low intensities and at low angles of beam incidence to avert risk of thermal alteration. Selected areas were examined with Philips (Eindhoven, The Netherlands) CM20, JEOL 200-CX, and JEOL 2010 transmission electron microscopes, all operated at 200 kV and equipped with detectors for energy dispersive spectrometry. These microscopes are able to form small electron probes for x-ray microanalysis (1 nm diameter is the minimum possible for 2010; typically, we used ≈5–10 nm), thus enabling reliable compositional analyses to be obtained. The 2010 microscope was equipped with a Gatan (Pleasanton, CA) slow-scan charge-coupled device (CCD) camera, which facilitated lattice imaging. Moderate electron beam intensities were used in TEM, and, whenever possible, short exposures of carbonate and sulfide phases to electrons were used to minimize radiation damage and avoid thermal volatilization. A minimum exposure method (17) was used when lattice imaging.

## Results

The orthopyroxene rock-mass is strongly deformed and unrecovered. More heterogeneously, it exhibits signs of alteration because of shock, which take several forms: breakdown to fibrous morphologies, formation of ≈100-nm-wide lamellae of glass of orthopyroxene composition, (glass of this composition was reported by Bell *et al.***), and transformation to clinopyroxene (18). The orthopyroxene glass indicates that shock pressures of 30–40 GPa were attained locally (19). Carbonate crystals show only local mild deformation, and they clearly crystallized around the orthopyroxene grains after the latter were strongly deformed and fractured. In fractured orthopyroxene, we found carbonate grains containing lenses and stringers of orthopyroxene glass, suggesting that the carbonate was fluid when the orthopyroxene melt was emplaced.

In magnesian regions of Mg-Fe-Ca carbonate grains (those with >80 mol % $MgCO_3$), we discovered periclase, MgO, occurring in ≈1-$\mu$m-sized patches of fine grains ≈3 nm in size. These patches usually exhibit evidence of a weak texture in electron diffraction (i.e., a tendency to be preferentially oriented) consistent with $\{111\}_{per}//(0001)_{carb}$, as found with the decomposition of calcite to lime, CaO (ref. 20) (Fig. 1 *a* and *b*). Less commonly, periclase occurs as individual crystals (typically

**Bell, M. S., Thomas-Keprta, K. L., Wentworth, S. J. & McKay, D. S. (1999) in *Proceedings of the 30th Lunar and Planetary Science Conference* (Lunar and Planetary Institute, Houston), no. 1951 (abstr.).

GEOPHYSICS

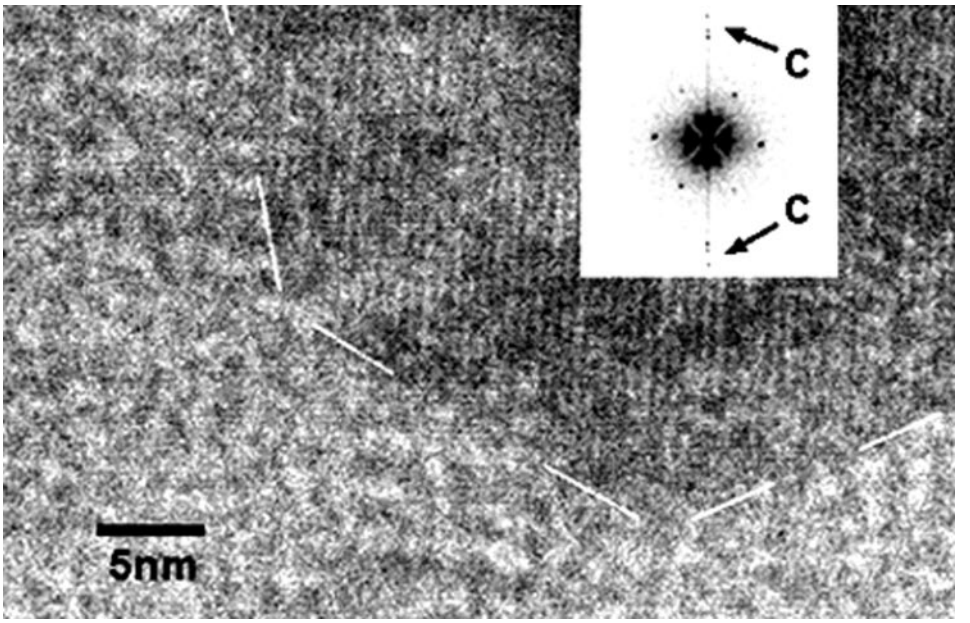


**Fig. 2.** Lattice image of part of a small embedded magnetite that was topotactic with the surrounding carbonate lattice (the white lines indicate the periphery of the magnetite). The carbonate close to the magnetite crystal is electron damaged but still shows (11$\bar{2}$6) lattice planes, spacing 0.167 nm (horizontal), that are parallel to (224) planes in the magnetite, spacing 0.171 nm. The simulated diffraction pattern (*Inset*) from the Fourier transform of a larger area including the magnetite crystal shows an hexagonal array of spots from the magnetite (imaging along a ⟨111⟩ zone axis) and weak spots (arrows, C) from the carbonate.

30–50 nm diameter) either enclosed within, or growing into, tiny voids in the carbonate (Fig. 1*c*). The MgO ring pattern (e.g., Fig. 1*b*) somewhat resembles that for $Fe_3O_4$ (e.g., Fig. 1*d*) because the lattice parameter of $Fe_3O_4$ is double that of MgO. Thus, positive identification of periclase requires diffraction rings at the $200_{MgO}$ and $220_{MgO}$ radii when iron is absent from the x-ray spectrum. In magnesian regions of massive carbonate, the patches of periclase are most easily recognized adjacent to fractures and open porosity. The nature and locations of the periclase are clear signs of *in situ* crystal growth during decomposition of the solid carbonate.

Magnetite crystals are found at numerous locations and in various forms in ferroan carbonate (carbonate with $<$80 mol % $MgCO_3$). The magnetite has four distinct occurrences: in optically opaque rims where it is agglomerated and intermixed with iron sulfide (which in our section appears to be mostly amorphous); as single crystals or small groups of crystals in cracks; as individual crystals in small voids in carbonate; or as crystals within solid carbonate. In the last two categories, the crystals are usually euhedral in form. Examples of these two categories are visible in Fig. 1*e*. As in the magnesian carbonate, the oxide inclusions are often associated with voids, and they are abundant adjacent to fractures and open porosity. Where magnetites and voids are especially abundant, both magnetite and fine-grained periclase are found.

We confirmed that magnetites growing in small voids and in microfractures frequently have epitaxial relationships with the carbonate (¶, 8). However, for the nanocrystals that are fully embedded in the ferroan carbonate, the crystallographic relationships are more extensive and very significant. These crystals constitute the most pertinent group to the mechanism of the formation of magnetite. We studied some of this group carefully by using lattice imaging methods to investigate the relationships between these magnetites and their host. The magnetites were too small to give good diffraction patterns, but we could simulate these from the lattice images by Fourier transforms. Our first discovery was that these magnetite crystals give good lattice images (e.g., Fig. 2), whichever zone axis of the carbonate is chosen for lattice imaging. This finding implies topotaxy (three-dimensional lattice continuity) rather than epitaxy. Therefore, this possibility was examined more systematically by imaging each crystal for two different carbonate zone axes. The first of these pairs of images invariably showed good continuity of the lattice planes across the magnetite-carbonate interfaces, although with some distortion. The second image was usually inferior in quality because of the damaging effect of the electron irradiation on the carbonate, rendering it less crystalline and more amorphous with time, even though we used a minimum dose technique (17). Nonetheless, we were able to confirm that the second image of each pair also exhibited lattice continuity at the magnetite-carbonate contacts, i.e., the interfaces are coherent or at least semicoherent. Such coherency is characteristic of the early stages of exsolution (e.g., ref. 21).

Fig. 3 *a* and *b* shows a pair of images from a magnetite crystal, with their corresponding diffraction patterns as *Insets* (actual patterns from the carbonate, not simulations derived from the lattice images). Because the lattice continuity is general (i.e., it does not depend on the direction of imaging), we became convinced that the fully embedded magnetites are topotactic with their carbonate host. To determine relationships between the lattices of the two phases, Fourier transforms of some of the high resolution images of magnetites in carbonate were used to simulate diffraction patterns. From several sets of data, we established the relationships between the two phases: $\{111\}_{mag}//(0001)_{carb}$ and $\{110\}_{mag}//\{11\bar{2}0\}_{carb}$. Although these relationships do not apply in every case, they are identical to those reported for the decomposition of calcite into lime (20) and are also consistent with our results for periclase. We have yet to identify any lime although we suspect it is present.

## Discussion

Periclase, unlike magnetite, which forms in a variety of igneous, metamorphic, and sedimentary rock types, is relatively uncommon in meteorites and earth rocks, and in nearly all cases it forms by thermal decomposition of dolomite or magnesian carbonate (e.g., refs. 22 and 23). In ALH 84001, many of the periclase

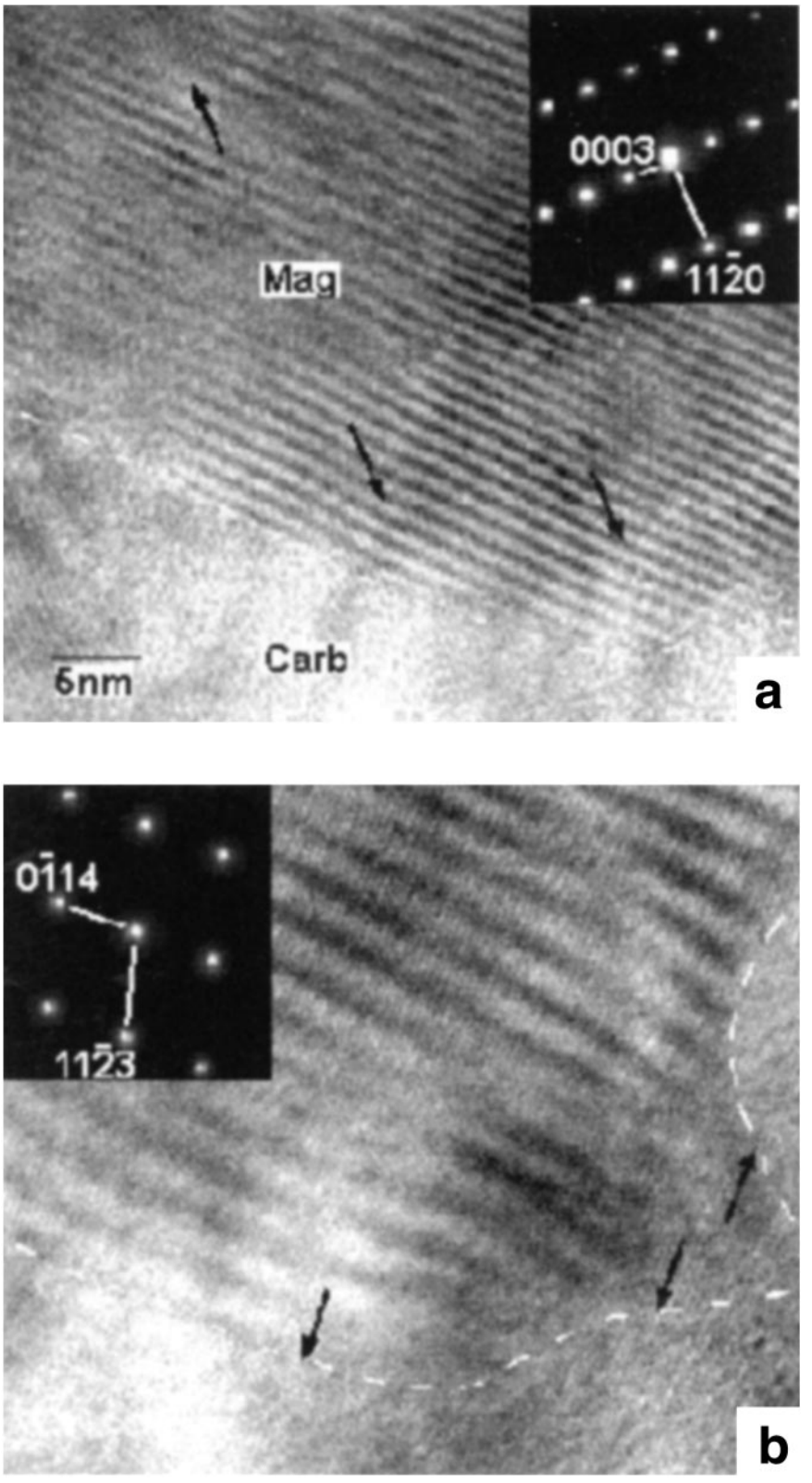


**Fig. 3.** Lattice images demonstrating the topotaxy of magnetite crystals that are fully embedded in ferroan carbonate. (*a*) Image of a magnetite crystal, larger than that of Fig. 2, viewed along a direction very close to the carbonate [$\bar{1}$100] zone axis, showing alignment and continuity of the (111) lattice planes in the oxide with the (0003) carbonate planes. The broken white lines locate the corresponding phase interface, whereas the arrows indicate where lattice planes within the magnetite align with and correspond to those in the carbonate. The strong 1-nm moiré fringes are caused by the close alignment of $(5\bar{1}3)_{mag}$ and $(11\bar{2}6)_{carb}$ planes (both tilted slightly off-axis and so not imaged), with interplanar spacings of 0.142 nm and 0.165 nm, respectively. (*Inset*) Zone axis diffraction pattern from the carbonate. (*b*) Image of the crystal seen in *a*, viewed along the carbonate [$\bar{6}$511] zone axis, which also shows continuity of the lattice planes across the phase interface (marked with broken white lines) where indicated with arrows. The 1.5-nm fringes covering the magnetite crystal are moiré fringes formed by $(171)_{mag}$ and $(21\bar{3},10)_{carb}$, with interplanar spacings of 0.118 nm and 0.109 nm respectively. (*Inset*) Zone axis diffraction pattern from the carbonate.



crystals are preferentially oriented with their close-packed layers of oxygen atoms oriented approximately parallel to those in the surrounding magnesian carbonate (Fig. 1*b*), as found in the decomposition of calcite to lime (20). Thus, the orientation and location of periclase crystals in ALH 84001 are strong evidence for *in situ* growth as a result of thermal decomposition of solid carbonate and loss of $CO_2$. In view of the localized shock melting of orthopyroxene and chronological evidence for major impact heating event around 4.0 Gyr (24), it is more likely that impact was the heat source for carbonate decomposition rather than deep burial and thermal metamorphism. Shock-induced formation of periclase from dolomite to yield a nanometer-sized

crystalline product has previously been reported (25). Lime is seldom apparent as a decomposition product of dolomites, although undoubtedly present in low volume fraction.

Our lattice imaging results show that many of the small magnetites outside the magnetite-rich rim (and probably all those that are entirely embedded in carbonate) have crystal lattices that are coherent with those of the host (Figs. 2 and 3). The crystallographic relationships between the magnetite and carbonate are characteristic of second phase crystals that have exsolved (i.e., precipitated in the solid state by means of diffusion). There are good examples in both metallic and nonmetallic systems (21, 26).

Magnetite and periclase are often associated with voids and microfractures in carbonate (Fig. 1*a*). In some regions, they are intermixed, and both oxides appear to have nucleated both homogeneously and heterogeneously. We suggest that their occurrence is entirely compatible with solid-state diffusion and exsolution as a result of thermal decomposition of carbonate. Because many oxides are not associated with voids, we infer that $CO_2$ was lost before oxide precipitation. Solid-state exsolution in crystals that are much larger than the effective diffusion length favors formation of numerous tiny single crystals and a tendency (although not an imperative) for them to grow in crystallographic relationships to the host carbonate lattice.

In our view, the species, sizes, and locations of oxide crystals in carbonate are simply functions of the Fe/Mg ratio, the abundance and nature of available nucleation sites, and variations in diffusivity because of the proximity of internal surfaces, vacancies, and other defects. The lower abundance and smaller grain size of periclase in magnesian carbonate compared with magnetite in the more ferroan carbonates is consistent with differences in stability.[††] Precipitation processes in supersaturated cooling solids commonly generate crystallites with characteristic faceted morphologies. Heterogeneous nucleation on internal surfaces and other defects is also common. These properties describe the observed carbonate-magnetite intergrowths very well.

At the optically opaque rims of carbonate crystals, where the most Fe-rich carbonate is located (27), there are agglomerates of magnetite particles, and the carbonate exhibits a subgrain structure. We infer that strain fields around the abundant magnetites interacted to produce a microstructure of small (≈100-nm-diameter) subgrains. (This dimension was determined by dark-field imaging.) Magnetites in the rims tend to be more diverse in size and more irregular in shape than other magnetites. Topotaxy with the decomposing host lattice is not favored because of its defective nature and probably also because the magnetites grew in a less controlled manner, as their diversity indicates.

Thomas-Keprta *et al.* (4, 5) argued that the elongated prismatic magnetites, which they inferred to be biogenic, are located mainly in the magnetite-rich rim where they found the carbonate to consist of randomly oriented crystals as small as 10 nm. We find to the contrary that carbonate in the magnetite-rich rim neither is fine grained nor lacks long-range order, as claimed, but rather that it appears to have been highly strained by the presence of the large volume-fraction of magnetite, imparting a microstructure of slightly misoriented subgrains ≈100 nm in size. Moreover, rim magnetite consists mostly of irregularly shaped crystals, consistent with growth in a highly strained matrix. We are convinced that euhedral magnetites largely occur as individual crystals in the carbonate, rather than in the densely populated magnetite-rich rim. Whereas the population outside the rim includes the rare whisker-like types, which are undoubtedly abiogenic (8, 9), it is mostly more-equiaxed faceted crystals with morphologies like the elongated prismatic crystals reported by Thomas-Keprta *et al.* (4).

The possibility that the whisker-like magnetites on microfractures (e.g., Fig. 1*e*) grew directly from a fluid or hot vapor, as Bradley *et al.* (9) suggested, is not excluded, but these magnetites may have grown by surface diffusion. Where chains of magnetite occur in ALH 84001, it is possible that they grew on ledges and kink sites on microfractures. Nucleation on such sites will be preferred above nucleation on defects like dislocations, or clustering on lattice sites. (Deposition on surfaces readily yields strings of precipitates that may appear curved at the microscopic level, because ledges and terraces commonly side-step on the atomic scale.)

Thomas-Keprta *et al.* (4, 5) offered several arguments against formation of magnetite in ALH 84001 by thermal decomposition of carbonate. They concluded that magnetites that formed this way should contain Mg and Mn, contrary to their analyses. However, experiments by Golden *et al.* (12) show that thermal decomposition of Mg-Fe-Ca carbonates can yield magnetite with undetectable Mg. Thomas-Keprta *et al.* (4) argued further that carbonate adjacent to magnetites that formed *in situ* by thermal decomposition should show chemical evidence for Fe mobilization, which they did not observe. However, our finding of topotactic magnetites and faceted voids (negative crystals) provides clear evidence for solid-state diffusion of ions and vacancies on scales of hundreds of nanometers. According to Thomas-Keprta *et al.* (4), magnetites that formed from the ALH 84001 carbonate should not contain the small concentrations of Al and Cr that they detected in irregular and whisker-shaped magnetite, because these elements have not been reported in the Martian carbonate. However, the ALH 84001 carbonates are notoriously impure: electron microprobe analyses of these carbonates show 0.01–1 wt. % Cr, Na, K, and Si (see ref. 28) and traces of Al. Even if these elements are located in minor phases, there are clearly sources of Al and Cr available to growing magnetite crystals. The lack of Al and Cr in elongated prismatic magnetites (4) is entirely consistent with our proposed formation mechanism. We should expect euhedral crystals that grow with coherent boundaries to be purer than irregular crystals growing with incoherent boundaries because the latter, unlike the former, readily accommodate impurities. Gibson *et al.* (29) argued against *in situ* formation of magnetite because Raman spectroscopic studies failed to detect CaO and MgO. However, our identification of periclase shows that earlier studies were not sensitive enough to detect these oxides. We suspect that CaO is also present sometimes, as an admixture; as yet, we have no certain proof. Given that the occurrences of magnetite in ALH 84001 carbonate can be explained perfectly well by established physico-chemical principles, there is no good reason why biogenic origins should be invoked and applied to a fraction of the isolated magnetites.

## Conclusions

Our results provide strong evidence that most and probably all of the magnetite grains in ALH 84001 are abiogenic in origin and that they formed because of shock-heating of the meteorite. Their occurrence is matched by the formation of periclase from the more magnesian fraction of the carbonates. The group of magnetites that are fully embedded in carbonate (which includes the size range of the putative biogenic magnetites) are topotactic with their host. We find $\{111\}_{mag}//(0001)_{carb}$ and $\{110\}_{mag}//\{11\bar{2}0\}_{carb}$ [the same as for lime, which is a decomposition product of calcium carbonate (20)]. This topotaxy is characteristic of exsolution in the solid state.

[††]Jones, J. H. & Schwandt, C. S. (1998) in *Proceedings of the 29th Lunar and Planetary Science Conference* [CD-ROM] (Lunar and Planetary Institute, Houston), no. 1425 (abstr.).

We have failed to find any sites where a special group of magnetites, like those identified by Thomas-Keprta *et al.* (4, 5) as probably biogenic, might be isolated or concentrated. Because a large proportion of the magnetite crystals are clearly attributable to decarbonation and decomposition of Fe-rich carbonate, it is highly improbable that a significant fraction was produced by a totally different, biogenic process and then intimately mixed with the former. The observations of chains of magnetite crystals (6) that have been offered as evidence of bacterial sources of magnetite can be explained by the well-documented mechanism of nucleation at terraces on internal carbonate crystal surfaces (e.g., microfractures).

We thank K. Z. Baba-Kishi for access to the JEOL 2010 microscope, G. K. H. Pang for invaluable assistance, and J. F. Kerridge for a useful discussion. We thank the National Aeronautics and Space Administration (NASA) Johnson Space Center Curatorial Facility and the Meteorite Working Group for the sample. We also thank three anonymous reviewers for constructive criticisms. This work was partially supported by NASA Grant NAG5-11591 to K. Keil and National Science Foundation Grant OPP-9714012 to E.R.D.S.

1. Borg, L. E., Connelly, J. N., Nyquist, L. E., Shih, C.-Y., Weissman, H. & Reese Y. (1999) *Science* **286,** 90–94.
2. Weiss, B. P., Kirschvink, J. L., Baudenbacher, F. J., Vali, H., Peters, N. T., MacDonald, F. A. & Wikswo, J. P. (2001) *Science* **290,** 791–795.
3. McKay, D. S., Gibson, E. K., Jr., Thomas-Keprta, K. L., Vali, H., Romanek, C. S., Clement, S. J., Chiller, X. D. F., Maechling, C. R. & Zare, R. N. (1996) *Science* **273,** 924–930.
4. Thomas-Keprta, K. L., Bazylinski, D. A., Kirschvink, J. L., Clement, S. J., McKay, D. S., Wentworth, S. J., Vali, H., Gibson, E. K., Jr., & Romanek, C. S. (2000) *Geochim. Cosmochim. Acta* **64,** 4049–4081.
5. Thomas-Keprta, K. L., Clement, S. J., Bazylinski, D. A., Kirschvink, J. L., McKay, D. S., Wentworth, S. J., Vali, H., Gibson, E. K., Jr., McKay, M. F. & Romanek, C. S. (2001) *Proc. Natl. Acad. Sci. USA* **98,** 2164–2169.
6. Friedmann, E. I., Wierzchos, J., Ascaso, C. & Winklhofer, M. (2001) *Proc. Natl. Acad. Sci. USA* **98,** 2176–2181.
7. Buseck, P. R., Dunin-Borkowski, R. E., Devouard, B., Frankel, R. B., McCartney, M. R., Midgley, P. A., Posfai, M. & Weyland, M. (2001) *Proc. Natl. Acad. Sci. USA* **98,** 13490–13495.
8. Bradley, J. P., Harvey, R. P. & McSween, H. Y., Jr. (1996) *Geochim. Cosmochim. Acta* **60,** 5149–5155.
9. Bradley, J. P., McSween, H. Y., Jr., & Harvey, R. P. (1998) *Meteorit. Planet. Sci.* **33,** 765–773.
10. Scott, E. R. D., Yamaguchi, A. & Krot, A. N. (1997) *Nature (London)* **387,** 377–379.
11. Golden, D. C., Ming, D. W., Schwandt, C. S., Morris, R. V., Yang, S. V. & Lofgren, G. E. (2000) *Meteorit. Planet. Sci.* **35,** 457–465.
12. Golden, D. C., Ming, D. W., Schwandt, C. S., Lauer, H. V., Socki, R. A., Morris, R. V., Lofgren, G. E. & McKay, G. A. (2001) *Am. Mineral.* **86,** 370–375.
13. Barber, D. J. & Wenk, H.-R. (1984) *Contrib. Mineral. Petrol.* **88,** 233–245.
14. Barber, D. J., Reeder, R. J. & Smith, D. J. (1985) *Contrib. Mineral. Petrol.* **91,** 82–92.
15. Barber, D. J. & Khan, M. R. (1987) *Mineral. Mag.* **51,** 71–86.
16. Barber, D. J. & Wenk, H.-R. (2001) *Eur. J. Mineral.* **13,** 221–243.
17. Barber, D. J., Freeman, L. A. & Smith, D. J. (1983) *Phys. Chem. Minerals* **9,** 102–108.
18. Ashworth, J. R. & Barber, D. J. (1976) in *Developments in Electron Microscopy and Analysis*, Proceedings of the Electron Microscopy and Analysis Group 1975 (Proc. EMAG 75), Bristol, U.K., ed. Venables, J. A. (Academic, London), pp. 517–520.
19. Leroux, H. (2001) *Eur. J. Mineral.* **13,** 253–272.
20. McTigue, J. W. & Wenk, H.-R. (1985) *Am. Mineral.* **70,** 1253–1261.
21. Putnis, A. & McConnell, J. D. C. (1980) *Principles of Mineral Behaviour* (Blackwell Scientific, Oxford).
22. Ikeda, Y. (1991) *Proc. Natl. Inst. Polar Res. Symp. Antarct. Meteorites* **4,** 187–225.
23. Chang, L. L. Y., Howie, R. A. & Zussman, J. (1995*) Rock-Forming Minerals*, (Longman, London) Vol. 5B, 2nd Ed.
24. Turner, G., Knott, S. F., Ash, R. D. & Gilmour, J. D. (1997) *Geochim. Cosmochim. Acta* **61,** 3835–3850.
25. Martinez, I., Deutsch, A., Schärer, U., Ildefonse, P., Guyot, F. & Agrinier, P. (1995) *J. Geophys. Res.* **100,** 15465–15476.
26. Aaronson, H. I. & Lee, J. K., eds. (1975) *Precipitation Processes in Solids* (Met. Soc. AIME, New York).
27. Treiman, A. H. & Keller, L. P. (2000) *Meteorit. Planet. Sci.* **35,** A158–9.
28. Scott, E. R. D., Krot, A. N. & Yamaguchi, A. (1998) *Meteorit. Planet. Sci.* **33,** 709–719.
29. Gibson, E. K., Jr., McKay, D. S., Thomas-Keprta, K. L., Wentworth, S. J., Westall, F., Steele, A., Romanek, C. S., Bell, M. S. & Toporski, J. (2001) *Precambrian Res.* **106,** 15–34.